

# Lung cancer combination therapy: doxorubicin and $\beta$ -elemene co-loaded, pH-sensitive nanostructured lipid carriers

This article was published in the following Dove Press journal:  
*Drug Design, Development and Therapy*

Chengsong Cao  
Qun Wang  
Yong Liu

Department of Oncology, Xuzhou  
Center Hospital, Xuzhou, Jiangsu,  
People's Republic of China

**Purpose:** Co-delivery of drugs to achieve the synergistic anticancer effect is a promising strategy for lung cancer therapy. The purpose of this research is to develop a doxorubicin (DOX) and  $\beta$ -elemene (ELE) co-loaded, pH-sensitive nanostructured lipid carriers (DOX/ELE Hyd NLCs).

**Methods:** In this study, DOX/ELE Hyd NLCs were produced by a hot homogenization and ultrasonication method and used for lung cancer treatment. In vitro and in vivo efficiency as well as toxicity of the system was evaluated on lung cancer cell lines and lung tumor-bearing mice.

**Results:** DOX/ELE Hyd NLCs had a particle size of 190 nm, with a PDI lower than 0.2. DOX/ELE Hyd NLCs exhibited a significantly enhanced cytotoxicity (drug concentration causing 50% inhibition was 7.86  $\mu$ g/mL), synergy antitumor effect (combination index lower than 1), and profound tumor inhibition ability (tumor inhibition ratio of 82.9%) compared with the non pH-responsive NLCs and single-drug-loaded NLCs.

**Conclusion:** Since the synergistic effect of the drugs was found in this system, it would have great potential to inhibit lung tumor cells and tumor growth.

**Keywords:** lung cancer, combination therapy, pH-sensitive, nanostructured lipid carriers, doxorubicin,  $\beta$ -elemene

## Introduction

Lung cancer is the leading cause of cancer death among men and the second leading cause of cancer death among women worldwide.<sup>1,2</sup> Low- and middle-income countries are now accountable for more than 50% of lung cancer deaths each year. Over the past 50 years, substantial progress has been made in all aspects of lung cancer including screening, diagnostic evaluation, surgery, radiation therapy, and chemotherapy.<sup>3</sup> Chemotherapy is effective based on the inhibition of the division of rapidly growing cancer cells, but unfortunately, it also affects normal cells with fast proliferation rates generating the characteristic side effects of chemotherapy.<sup>4</sup> Novel nanoparticle formulations of cytotoxic chemotherapy drugs can enhance pharmacokinetic characteristics and facilitate passive targeting of drugs to tumors via the enhanced permeability and retention effect, thus mitigating toxicity.<sup>5</sup> These carriers include vesicular and particulate systems such as liposomes, niosomes, transfersomes, ethosomes, micelles, dendrimers, and polymeric, protein and lipid nanoparticles.<sup>6</sup>

Correspondence: Yong Liu  
Department of Oncology, Xuzhou Center  
Hospital, Number 199 Jiefang Road,  
Xuzhou, Jiangsu 221009, People's  
Republic of China  
Email liuyxz7011@sohu.com

Lipid nanoparticles are colloidal particles composed of a biocompatible and biodegradable lipid matrix that is solid at body temperature and exhibits a size range in between 100 and 400 nm.<sup>7</sup> Among all types of lipid nanoparticles, nanostructured lipid carriers (NLCs) constituted of blends of lipids in solid, and liquid state can be considered as the last generation.<sup>8</sup> They are produced by controlled mixing of solid lipids with spatially incompatible liquid lipids, leading to a specific nanostructure to accommodate drugs and thus achieve higher loading capacity.<sup>9</sup> Based on their good biocompatibility and stability, high drug loading, and low preparation cost, NLCs systems have become promising carriers for improving the bioavailability of some of the poorly water-soluble drugs.<sup>10</sup> For example, doxorubicin (DOX) was loaded in NLCs and used as promising targeted drug delivery systems for lung cancer therapy by several researchers.<sup>11–13</sup> Furthermore, lipid nanoparticles with structures that respond to external stimuli (including pH, light, and enzyme activities) have attracted considerable attention in the field of cancer therapy.<sup>14</sup> The pH in tumor tissues is far more acidic (pH =5–6) than the wider physiological environment (pH =7.4).<sup>15</sup> Thus pH-sensitive nanoparticles represent an effective strategy for cancer therapies. In this study, acid-sensitive hydrazone (Hyd) linkage contained NLCs were used. When the NLCs were delivered to the acidic tumor site, Hyd linkage may decompose and enhance the drug release.

In China, herbal medicine is frequently combined with chemotherapy in the treatment of lung cancer.<sup>16</sup>  $\beta$ -elemene (1-methyl-1-vinyl-2,4-diisopropenyl-cyclohexane) (ELE) is an antitumor agent extracted from the Chinese medicinal plant, *Radix Curcumae*. ELE has moderate antitumor activity and is mainly used as an adjunctive drug to enhance the efficacy, reduce the toxicity of chemoradiotherapy, and reverse drug resistance.<sup>17</sup> Previous studies have shown that ELE exhibited anti-cancer effects in many cancer cells, especially lung cancer cells by inducing apoptosis.<sup>18</sup> ELE has been reported to radiosensitize lung cancer cells by enhancing DNA damage and inhibiting DNA repair through up-regulating the expression of P53.<sup>19</sup> ELE was also described to decrease the expression of *P*-glycoprotein (*P*-gp), inhibit the *P*-gp-dependent drug efflux, and increase the intracellular concentration of anticancer drugs, leading to the reversal of drug resistance in lung cancer cells.<sup>20</sup> Therefore, we used ELE along with DOX to achieve the synergistic anticancer effect on lung carcinoma.

In the present study, DOX and ELE co-loaded, pH-sensitive nanostructured lipid carriers (DOX/ELE Hyd NLCs) were produced and used for lung cancer treatment. In vitro and in vivo efficiency as well as toxicity of the system was evaluated on lung cancer cell lines and lung tumor-bearing mice.

## Material and methods

### Chemicals and reagents

Doxorubicin hydrochloride (DOX·HCl), ELE triethylamine (TEA), and dimethyl sulfoxide (DMSO) were purchased from Sigma-Aldrich (Shanghai, China). Compritol® 888 ATO was provided by Gattefossé (Saint-Priest, Lyon, France). Miglyol® 812 was purchased from Caelo (Hilden, Germany). Lecithin was obtained from Lipoid GmbH (Ludwigshafen, Germany). Methoxy (polyethylene glycol) 2000- hydrazone- 1,2-distearoyl-sn-glycero-3-phosphoethanolamine (mPEG-Hyd-DSPE) and mPEG-DSPE were provided by Xi'an Ruixi Biological Technology Co., Ltd. (Xi'an, China). Fetal bovine serum (FBS), Dulbecco's modified Eagle's medium (DMEM), and 3-(4,5-dimethyl-2-thiazolyl)-2,5-diphenyl-2-H-tetrazolium bromide (MTT) were purchased from Invitrogen Corporation (Carlsbad, CA). ELE injection was provided by Dalian Holley Kingkong Pharmaceutical Co., Ltd (Dalian, China). All other reagents and chemicals were of analytical grade or high-performance liquid chromatography grade and were used without further purification.

### Cells and animals

A549 lung cancer cells (A549 cells, lot: 60157386) and human embryo lung cells (MRC-5 cells, lot: 62385617) were purchased from American Type Culture Collections (Manassas, VA). DOX-resistant A549 cells (A549/ADR cells, lot: 18032501) were provided by Shanghai MEIXUAN Biological Technology Co, Ltd (Shanghai, China).<sup>21</sup> Cells were grown in DMEM (glucose concentration lower than 4500mg/L) containing 10% inactivated FBS and 1% penicillin-streptomycin and maintained in a humidified incubator at 37°C with 5% CO<sub>2</sub>.<sup>22</sup>

Male C57BL/6 mice (6 weeks old) were purchased from Beijing Vital River Laboratory Animal Technology Co., Ltd. (Beijing, P.R.C.) and raised under conventional conditions with a 12 h light/dark cycle, constant temperature (25°C), and humidity (60%). Animal experiments were performed according to the National Institutes of Health guide for the care and use of laboratory animals

(NIH Publications No. 8023, revised 1978) and approved by the ethics committee of Xuzhou Center Hospital.

## Preparation of DOX/ELE Hyd NLCs

DOX/ELE Hyd NLCs (Figure 1A) were prepared by a hot homogenization and ultrasonication method.<sup>23</sup> Firstly, DOX·HCl was stirred with three equivalents molar ratio of TEA in DMSO overnight to obtain the DOX base. Compritol® 888 ATO (100 mg) and Miglyol® 812 (150 mg) were mixed and heated to about 70°C until melted; then, DOX (100 mg) and ELE (50 mg) was added to the mixture and stirred to form the oil phase. mPEG-Hyd-DSPE (100 mg), lecithin (50 mg), and Tween® 80 (1%) were dissolved in water (100 mL) and heated to about 70°C to get the aqueous phase. Aqueous phase was then added to the oil phase, homogenized at 15,000 rpm for 2 min, and ultrasonicated using an ultrasonication probe during 2.5 min at 70% amplitude. The mixture was then cooled to 2–8°C using an ice-water bath.

DOX and ELE co-loaded NLCs do not contain pH-sensitive Hyd (DOX/ELE NLCs) and were prepared by the same method using mPEG-DSPE instead of mPEG-Hyd-DSPE. DOX single-drug-loaded pH-sensitive NLCs (DOX Hyd NLCs) were prepared by the same method using 200 mg of DOX and without adding ELE. ELE single-drug-loaded pH-sensitive NLCs (ELE Hyd NLCs) were prepared by the same method using 200 mg of ELE and

without adding DOX. Blank pH-sensitive NLCs (Hyd NLCs) were prepared by the same method without adding ELE and DOX. DOX- and ELE-contained injection (DOX/ELE INJ) was prepared by dissolving DOX·HCl (200 mg) in ELE injection (containing 200 mg of ELE).

## Characterization of entrapment efficiency and drug loading

The untrapped free DOX and ELE was separated from the drug entrapped in the NLCs by an ultrafiltration method.<sup>24</sup> Briefly, after diluting with Tween® 80 containing phosphate buffer solution (PBS), NLCs were centrifuged at 10,000 rpm for 15 min using centrifugal filter tubes (molecular weight cutoff: 10,000; Nanosep MF; Pall Corporation, Port Washington, NY). The free DOX was collected in the under-layer solution. The DOX content was determined with F-4500 fluorescence spectrophotometer (emission wavelength: 480 nm, excitation wavelength: 556 nm, Hitachi, Tokyo, Japan).<sup>25</sup> The amount of ELE was measured using gas chromatography spectrometry (GC) under the following conditions: Agilent 7890A GC system coupled with a flame ionization detector and an Agilent 19091–413 HP-5 capillary column (30 m × 0.32 mm × 0.25 μm), with the temperature set to increase from 60°C to 200°C at a rate of 10°C/minute. The entrapment efficiency (EE) and drug loading (DL) were mathematically calculated using equations:

$$EE (\%) = (\text{total amount of drugs} - \text{the amount of untrapped drugs}) / \text{total amount of drugs} \times 100.$$

$$DL (\%) = (\text{total amount of drugs} - \text{the amount of untrapped drugs}) / \text{total amount of lipids} \times 100.$$

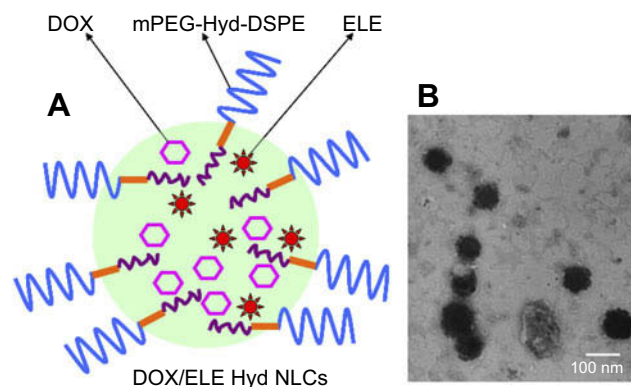


**Figure 1** Scheme graph (A) and TEM image (B) of doxorubicin and  $\beta$ -elemene co-loaded, pH-sensitive nanostructured lipid carriers (DOX/ELE Hyd NLCs).

## Diameter, polydispersity index, and zeta potential

NLC suspensions were diluted with PBS (pH 7.4) to an appropriate concentration for the measurement. Hydrodynamic diameter, polydispersity index (PDI), and zeta potential of NLCs were measured by a Zetasizer Nano series ZS90 (Malvern Instruments, Malvern, UK) at room temperature.<sup>26</sup> The surface morphology of the DOX/ELE Hyd NLCs was examined by transmission electronic microscopy (TEM) using JEM-1200EX transmission electron microscope (JEOL Ltd., Tokyo, Japan).

## Plasma stability

The plasma stability of NLCs in serum was examined in FBS.<sup>27</sup> NLC suspensions were incubated with 10% FBS (v/v) solution at 37°C under 100 rpm gentle stirring for 1, 2, 4, 8, 12, 24, 48, and 72 hrs. Their diameter and PDI were measured at each time point to determine the stability.

## In vitro drug release

In vitro drug release from NLCs was investigated using the dialysis method.<sup>28</sup> NLC suspensions (2 mL) were placed in dialysis bags with a molecular weight cutoff of 3.5 kDa. The dialysis bags were immersed in acetate buffer (50 mL) at the pH of 5.5 and 7.4, with constant shaking (37°C, 100 rpm). At predetermined time points, 300 µL of the dialysis solution was withdrawn for analysis, and the same amount of fresh buffer was added. The amount of released drugs was determined by the method described in “Characterization of entrapment efficiency and drug loading” section.

**Cellular uptake** A549/ADR cells were seeded into coverglass-containing 24-well plates at a density of  $2 \times 10^4$  cells per well and incubated overnight. Coumarin-6-loaded NLCs were prepared with the coumarin-6 to lipids ratio of 1: 2,000 (w/w).<sup>29</sup> Coumarin-6-loaded NLCs (200 mg/mL) were added to the A549/ADR cells which were equilibrated with Hank's buffered salt solution (37°C, 1 hr) in advance. The medium was removed after incubated for the determined time (2, 4, and 8 hrs), and the wells were washed three times with cold PBS solution and detached with trypsin/EDTA. Then, the cells were centrifuged at 1500 rpm, 4°C for 5 min and re-suspended in 300 µL of PBS and directly introduced to a BD FACSCalibur flow cytometer (Becton, Dickinson and Company, Franklin lakes, NJ). The fluorescence intensity at 8 he was measured at an excitation wavelength of 488 nm using an inversion fluorescence microscope (OLYMPUS, Tokyo, Japan) and the picture was captured.

## Cytotoxicity and synergistic effect

Cytotoxicity of NLCs was investigated using an MTT assay.<sup>30</sup> A549, A549/ADR or MRC-5 cells were seeded with  $1 \times 10^4$  cells per well in 96-well plates and grown overnight at 37°C in a 5% CO<sub>2</sub> incubator. NLCs and DOX/ELE INJ at various concentrations were added into each well and incubated for 72 hr. At that point, they were incubated with MTT for 4 hr, followed by an additional

4 hr incubation with DMSO to dissolve the MTT formazan crystals. The absorbance of each sample was measured at 570 nm using a microplate reader (Model 680, Bio-Rad Laboratories Inc., Philadelphia, PA). Cells without the addition of MTT reagents were used as a blank control.

The drug concentration causing 50% inhibition (IC<sub>50</sub>) was calculated and combination index (CI) was measured to study the synergistic effect in the DOX/ELE Hyd NLCs system. CI values were calculated using equations:  $CI_{50} = C_{DOX}/C_{50-DOX} + C_{ELE}/C_{50-ELE}$ .  $C_{DOX}$  and  $C_{ELE}$  represent the concentration of DOX and ELE in the combination system at the IC<sub>50</sub> value, separately.  $C_{50-DOX}$  and  $C_{50-ELE}$  represent the IC<sub>50</sub> value of DOX alone and ELE alone, respectively.  $CI_{50} < 1$  means synergism and  $> 1$  represent antagonism. The CI<sub>50</sub> values curves were drawn according to Fa (the fraction of affected cells). Fa values between 0.2 and 0.8 are considered validate.

## In vivo tissue distribution

Tumor xenografts were produced by subcutaneously injected A549/ADR cells suspension ( $10^6$  cells suspended in 100 µL 0.9% normal saline) into the right flank of mice.<sup>31</sup> When tumors reached approximately 100 mm<sup>3</sup>, the mice were divided to 7 groups (8 mice pre group) and were administered a single dose of 200 µL DOX/ELE Hyd NLCs, DOX/ELE NLCs, DOX Hyd NLCs, ELE Hyd NLCs, Hyd NLCs, DOX/ELE INJ (50 mg/kg), and 0.9% normal saline by a tail vein injection. Mice were sacrificed at 1 and 23 hr following injection, and tissue samples were digested by concentrated nitric acid overnight at room temperature. After addition of 2 mL of distilled water, drugs were extracted from the resultant mixture using 3 mL of methanol. The extract was partitioned into two layers by centrifugation at  $1,000 \times g$  for 10 mins at 4°C and the supernatant liquid was separated. The concentration of drugs was measured by the method described in section 2.4.

## In vivo anticancer activity

The same tumor xenografts, groups, and injection amount were used as described in “In vivo tissue distribution” section. The difference is the samples were injected every three days. Following drug administration, tumor growth was measured every three days.<sup>32</sup> The tumor volume (TV) was calculated according to the equation:  $TV (mm^3) = (\text{length} \times \text{width}^2)/2$ . On the 18th day after the first administration, the mice were killed and the tumor of each mouse was captured, weighed, and tumor inhibition



**Table 1** EE and DL of NLCs (mean  $\pm$  SD, n=3)

| NLCs             | DOX EE (%)     | ELE EE (%)     | DOX DL (%)     | ELE DL (%)    |
|------------------|----------------|----------------|----------------|---------------|
| DOX/ELE Hyd NLCs | 89.3 $\pm$ 3.9 | 87.7 $\pm$ 4.2 | 12.1 $\pm$ 0.8 | 5.7 $\pm$ 0.7 |
| DOX/ELE NLCs     | 91.8 $\pm$ 4.6 | 86.9 $\pm$ 3.8 | 10.8 $\pm$ 0.9 | 4.9 $\pm$ 0.6 |
| DOX Hyd NLCs     | 90.5 $\pm$ 3.7 | –              | 9.6 $\pm$ 1.1  | –             |
| ELE Hyd NLCs     | –              | 88.6 $\pm$ 4.9 | –              | 5.2 $\pm$ 0.8 |

**Abbreviations:** DL, drug loading; EE, entrapment efficiency; DOX/ELE Hyd NLCs, doxorubicin and  $\beta$ -elemene co-loaded, pH-sensitive nanostructured lipid carriers.

ratios (TIR) were calculated according to the equation: TIR (%) = (Tumor weight of the control – tumor weight of the treated)/(tumor weight of the control)  $\times$  100.

## Statistical analysis

The data was presented as the mean  $\pm$  standard deviation. The multiple groups were compared using a one-way analysis of variance and between two groups by Student's *t* test analysis. *P*-value of less than 0.05 was considered statistically significant.

## Results

### Characterization of NLCs

The EE and DL of NLCs are summarized in Table 1. The DOX and ELE EE of NLCs was around 90%. However, the DOX and ELE DL of NLCs were different: DOX and DOX DL were about 10% and 5%, respectively.

Mean diameters of various kinds of NLCs were around 190 nm, with PDIs lower than 0.2 (Figure 2). The zeta potentials of NLCs are between  $-30.9$  and  $-41.3$  mV. TEM image of DOX/ELE Hyd NLCs is presented in Figure 1B.

Stability of NLCs in plasma was evaluated and simulated in 10% FBS at 37°C for 72 hrs. NLCs showed no significant size and PDI changes during the 72-hr test which could prove the plasma stability of the systems (Figure 3).

### In vitro release behavior

In vitro release behaviors of pH-sensitive DOX/ELE Hyd NLCs and non-Hyd containing DOX/ELE NLCs at pH 5.5 and 7.4 were measured (Figure 4). The release of DOX and ELE from DOX/ELE Hyd NLCs was faster at pH 5.5 than at pH 7.4. In contrast, drug release of DOX/ELE

NLCs followed the same pattern at pH 5.5 and 7.4. This could be the evidence that the pH-sensitive NLCs could trigger by the acidic pH and release the drugs faster from the carriers.

### Cellular uptake

Cellular uptake efficiency of NLCs was illustrated by coumarin-6-loaded NLCs in A549/ADR cells. As shown in Figure 5A, cellular uptake efficiency of NLCs increased along with time. Around 70% of uptake was observed at 8 hr posttreatments. DOX/ELE Hyd NLCs exhibited more obvious fluorescence than DOX/ELE NLCs at 8 hr post treatments (Figure 5B), which is in accordance with the results in Figure 5A.

### Cytotoxicity and synergistic effect

In vitro cytotoxicity of NLCs was evaluated on A549, A549/ADR, and MRC-5 cells (Figure 6). On both A549 and A549/ADR cells at all the studied drug concentrations, the cytotoxicity of DOX/ELE Hyd NLCs was higher than DOX/ELE NLCs; DOX/ELE NLCs were higher than DOX/ELE INJ ( $P < 0.05$ ). DOX/ELE Hyd NLCs exhibited better cell inhibition effect than single-drug-loaded DOX Hyd NLCs and ELE Hyd NLCs ( $P < 0.05$ ). DOX-containing formulations showed lower efficacy on A549/ADR cells than A549 cells, but ELE could help with the system to achieve cytotoxicity.  $CI_{50}$  was measured to validate the synergistic effect of DOX and ELE in the NLCs and injection systems. The  $CI_{50}$  value was  $< 1$  when  $0.2 < Fa < 0.8$ , indicating the pronounced synergy effect of the DOX/ELE Hyd NLCs. Drugs contained NLCs, and DOX/ELE INJ did not show a significant difference in MRC-5 cells.

### In vivo tissue distribution

In vivo tissue distribution of NLCs and drugs injection in tumor xenografts are compared in Figure 7. NLC systems exhibited higher drug concentration than DOX/ELE INJ in the tumor tissue at both 1 he and 24 he ( $P < 0.05$ ). At 1 h after administration, NLCs showed a lower distribution in heart and kidney compared with DOX/ELE INJ ( $P < 0.05$ ). This may reduce the systematic toxicity of the drugs.

### In vivo anticancer activity

In vivo anticancer activity was presented as tumor growth curves and tumor images of each group (Figure 8). The results indicated that treatment with drugs loaded NLCs groups showed profound suppressed tumor growth than

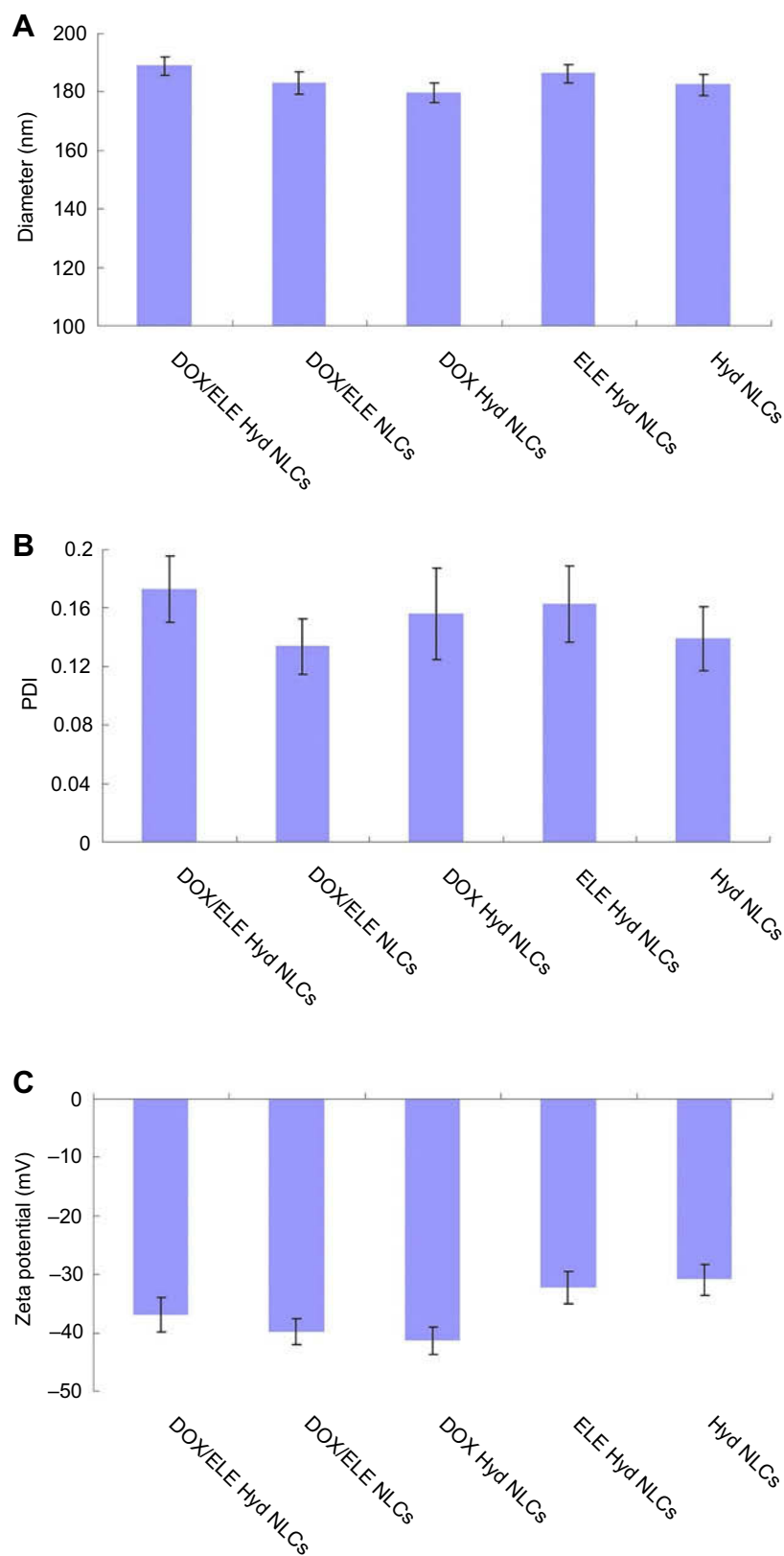


**Figure 2** Particle sizes (A), polydispersity indices (B), and zeta potentials (C) of NLCs. Data are presented as mean  $\pm$  SD, n=10.  
**Abbreviation:** DOX/ELE Hyd NLCs, doxorubicin and  $\beta$ -elemene co-loaded, pH-sensitive nanostructured lipid carriers.

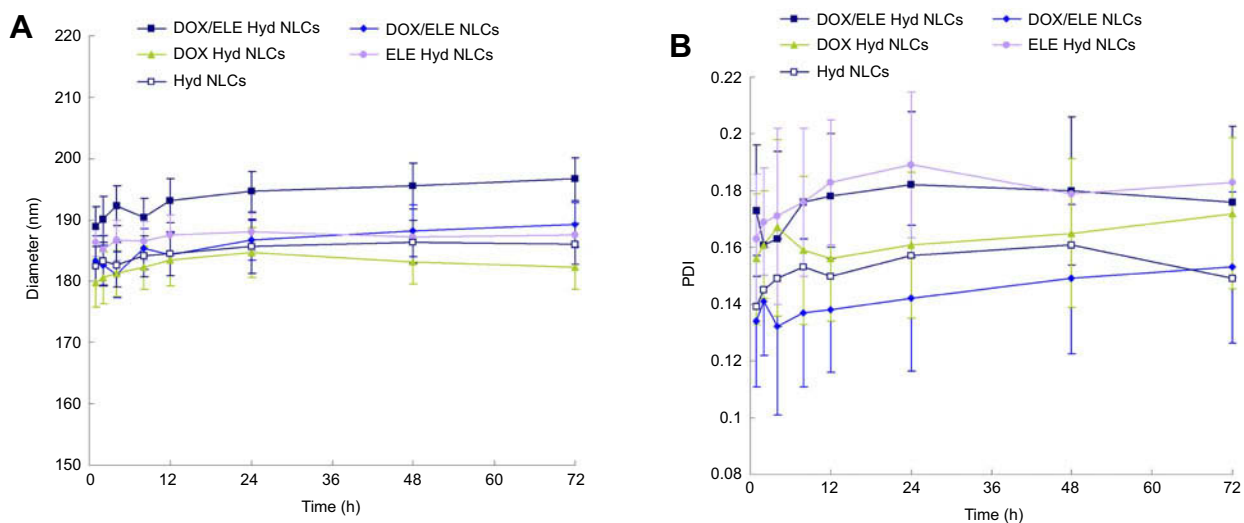


**Figure 3** Plasma stability of NLCs evaluated simulated in 10% FBS. NLCs showed no significant size (A) and PDI (B) changes during the 72-hr test. Data are presented as means  $\pm$  SD, n=10.

**Abbreviations:** PDI, polydispersity index; DOX/ELE Hyd NLCs, doxorubicin and  $\beta$ -elemene co-loaded, pH-sensitive nanostructured lipid carriers.

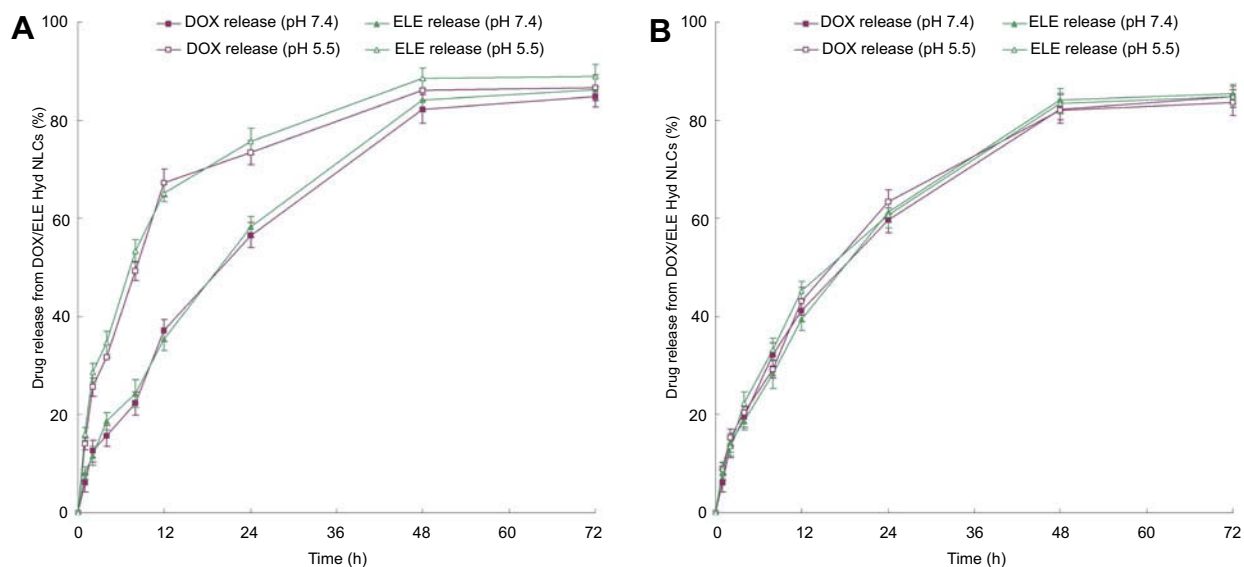


**Figure 4** In vitro release behavior of pH-sensitive DOX/ELE Hyd NLCs (A) and DOX/ELE NLCs (B) at pH 5.5 and 7.4. Data are presented as means  $\pm$  SD, n=3.

**Abbreviation:** DOX/ELE Hyd NLCs, doxorubicin and  $\beta$ -elemene co-loaded, pH-sensitive nanostructured lipid carriers.

that of DOX/ELE INJ ( $P < 0.05$ ). The tumor volume of DOX/ELE Hyd NLCs at day 18 was  $293 \text{ mm}^3$ , which is significantly smaller compared with DOX/ELE NLCs ( $592 \text{ mm}^3$ ), DOX Hyd NLCs ( $650 \text{ mm}^3$ ), and ELE Hyd NLCs ( $912 \text{ mm}^3$ ). Tumor inhibition ratios of all the formulations were summarized, and DOX/ELE Hyd NLCs exhibited the most remarkable TIR of 82.9% (Table 2).

## Discussion

In this study, pH-sensitive nanocarriers were designed using an acid-sensitive hydrazone (Hyd) linkage

containing mPEG-Hyd-DSPE. NLCs contain the pH-cleavable mPEG-Hyd-DSPE which should be stable at neutral physiologic conditions in the extracellular compartment. After entering environments with decreasing pH, such as the extracellular space of some tumors, the complex would be expected to release more drugs upon cleavage of the pH-sensitive hydrazone bond.<sup>33</sup> According to the literature, curcumin-loaded pH-sensitive hybrid lipid/block copolymer nanosized drug delivery systems were developed by Jelezova et al, and they achieved more drug release in lower pH.<sup>34</sup> In vitro release assays

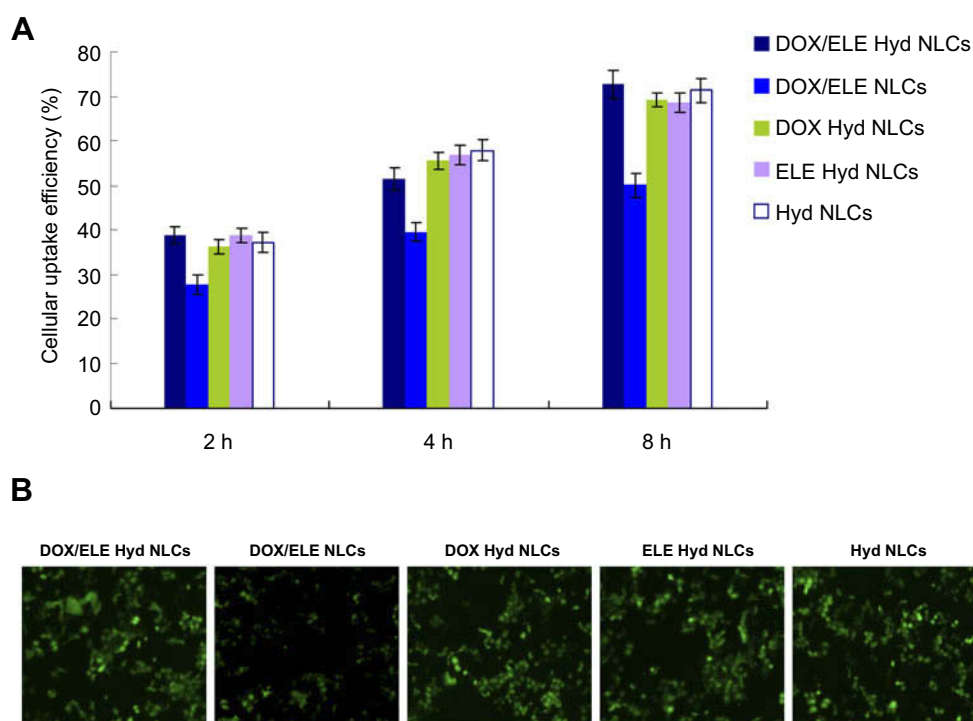


**Figure 5** Cellular uptake efficiency of NLCs was illustrated by coumarin-6-loaded NLCs in A549/ADR cells: flow cytometry results (A) and microscopy images. (B) Data are presented as means  $\pm$  SD, n=6.

**Abbreviation:** DOX/ELE Hyd NLCs, doxorubicin and  $\beta$ -elemene co-loaded, pH-sensitive nanostructured lipid carriers.

showed that drug release from pH-sensitive DOX/ELE Hyd NLCs was rapid at pH 5.5, while it was much slower at pH 7.4. This could be the evidence that the pH-sensitive NLCs could be triggered by the acidic pH and release the drugs faster from the carriers.

Particle size, zeta potential, and plasma stability are important characteristics of drugs-loaded nanocarriers.<sup>35</sup> The size and zeta potential of NPs not only determine their colloidal stability but also influence the effectiveness of their interaction with cell membranes, which is the pivotal step for successful cellular uptake. Particle sizes of various kinds of NLCs were around 190 nm. These nano-sized nanocarriers have advantages in comparison to systemic chemotherapy. Nanoparticles are known to exploit the enhanced permeability and retention (EPR) effect for targeting tumors, thereby increasing tumor drug concentrations while minimizing systemic toxicity.<sup>36</sup> Additionally, due to the lipid structure of NLCs, they had good biocompatibility with the cell membrane of the cancer cells.<sup>37</sup> The plasma stability of NLCs was tested in serum-included media. NLCs exhibited no obvious changes in size and PDI after mixing with serum media, which may contribute to the maintenance of colloidal stability even in serum-included media.<sup>38</sup> pH-sensitive micelles based on acid-labile pluronic F68-curcumin conjugates were

constructed by Fang et al for improved tumor intracellular drug delivery. The cellular uptake of the micelles was higher than free drug formulation.<sup>39</sup> The cellular uptake of different formulations was evaluated in A549/ADR cells. High cellular uptake efficiency of NLCs was observed at 8 hr posttreatments. This may attribute to the lipid nature of the NLCs that could well integrate with the cell membrane, thus induce good cell uptake results.<sup>40</sup> The cellular uptake results obtained correlated with cytotoxicity results.

In vitro cytotoxicity of NLCs was evaluated on both A549 and A549/ADR cells. Higher cell toxicity of drug-loaded NLCs was observed than DOX/ELE INJ. The use of multiple drugs in combination has possible favorable outcomes, such as synergism, additive, and antagonism.<sup>41</sup> Evaluation of drug–drug interaction is important in all areas of medicine, particularly in cancer chemotherapy where combination therapy is commonly used. In order to determine the possible effect of the drug combination, mathematical model-based method has been introduced. DOX and ELE co-loaded NLCs have a better ability and showed obvious synergism effect than the single-drug-loaded NLCs. CI analyses are the most popular methods for evaluating drug interactions in combination cancer chemotherapy. In this



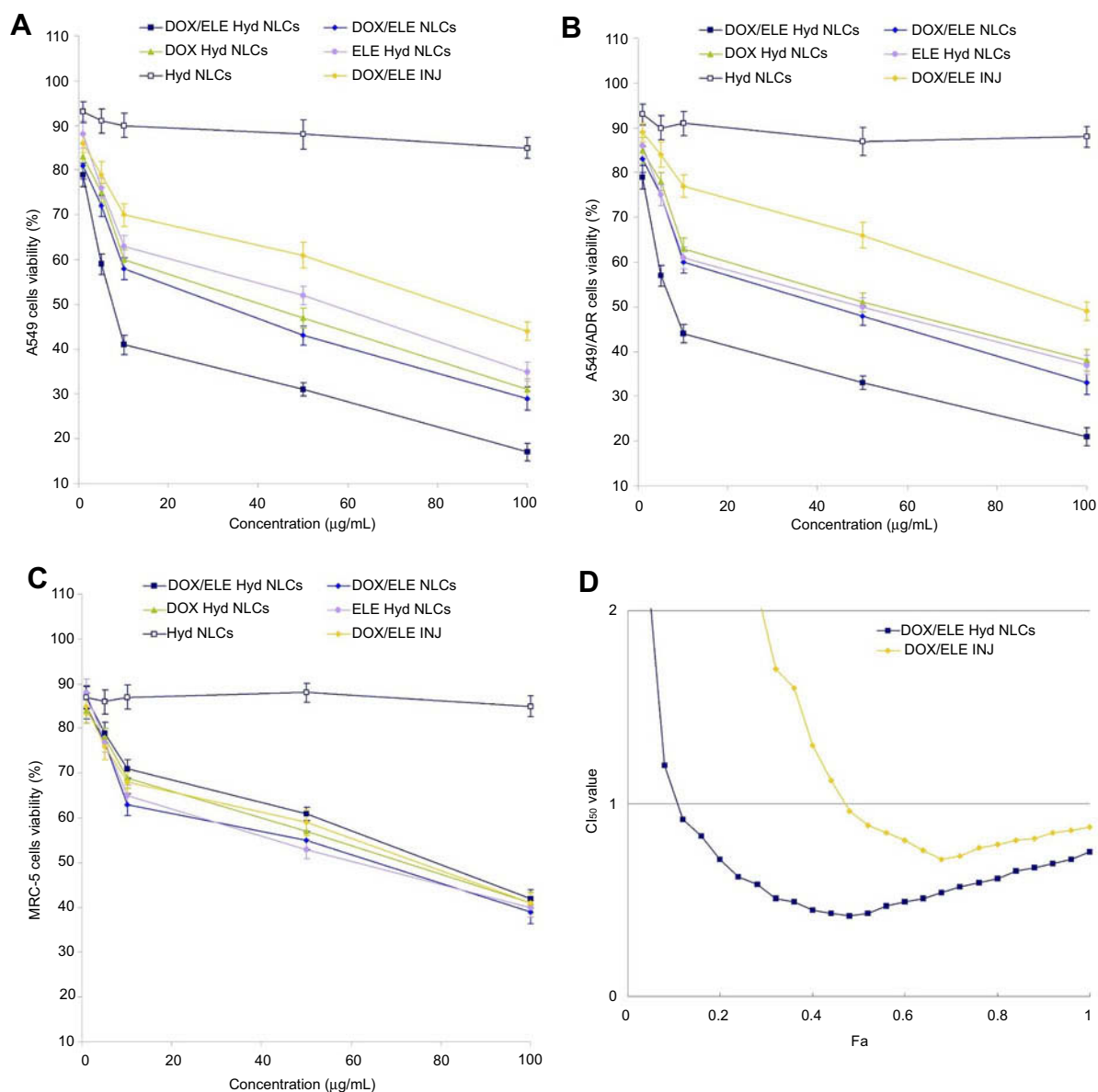


**Figure 6** In vitro cytotoxicity of NLCs was evaluated on both A549 (A), A549/ADR cells (B), and MRC-5 cells (C).  $CI_{50}$  was measured to validate the synergistic effect (D). Data is presented as mean  $\pm$  SD,  $n=6$ .

**Abbreviation:** DOX/ELE Hyd NLCs, doxorubicin and  $\beta$ -elemene co-loaded, pH-sensitive nanostructured lipid carriers.

study,  $CI_{50}$  was measured to validate the synergistic effect of DOX and ELE in the NLCs and injection systems. The  $CI_{50}$  value was  $<1$  when  $0.2 < Fa < 0.8$ , indicating the pronounced synergy effect of the DOX/ELE Hyd NLCs.

In vivo tissue distribution behavior of NLCs and injection was investigated in A549/ADR cells bearing lung tumor xenografts. High accumulation of NLCs was found in the tumor tissue than in other normal tissues, which supported the preferential accumulation of NLCs in the tumor based on the EPR effect.<sup>42</sup> Drug concentrations of NLCs in the tumor tissue remained high until 24 he after

injection, indicate the long-circulating behavior of the NLCs. The long-circulating effect is attributed to the presence of PEG chains on the surface of particles, which provided stealth effect to the LPNs. Ding et al introduced an efficient PEGylated liposomal nanocarriers containing pH-sensitive hydrazone bond for enhancing tumor-targeted drug delivery.<sup>43</sup> They found that the in vivo tumor accumulation of drugs in PEGylated liposomal nanocarriers were higher. This is in line with the results with the present study.

In vivo antitumor efficacy of NLCs investigated on lung tumor mice model demonstrated that DOX/ELE Hyd NLCs showed the strongest antitumor effect. Higher TIR of drug-

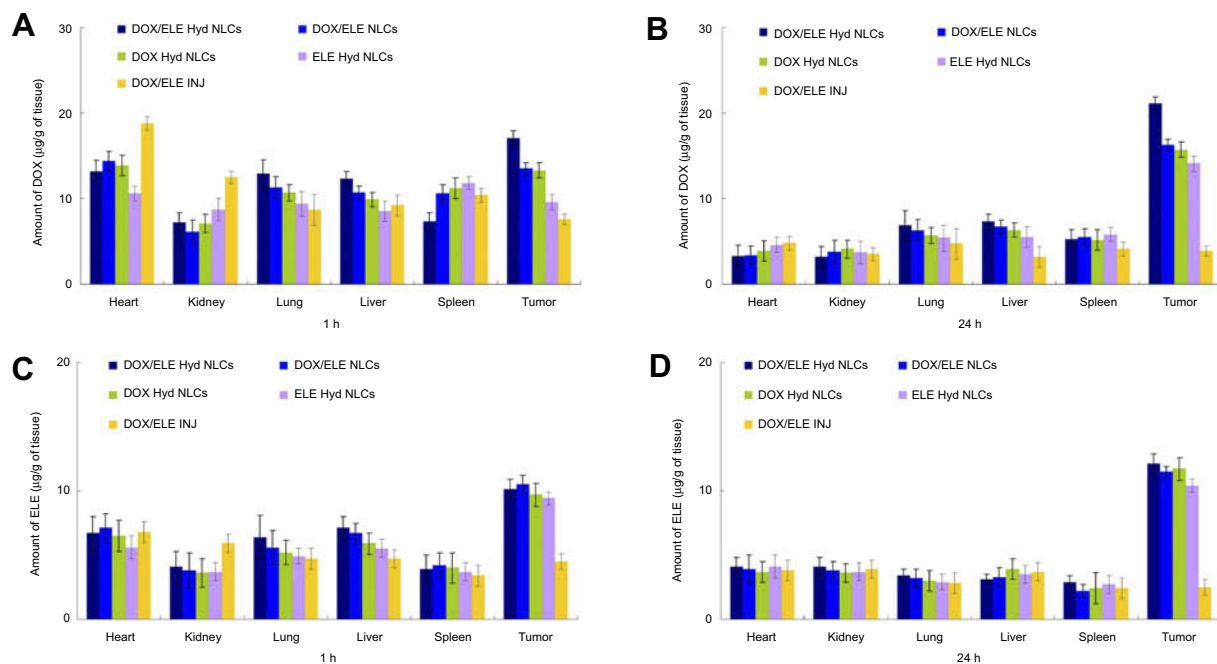


**Figure 7** In vivo tissue distribution of NLCs and drugs injection (INJ) in tumor xenografts: DOX distribution at 1 hr (A) and 24 hr (B); ELE distribution at 1 hr (C) and 24 hr (D). Data is presented as means ± SD, n=8.

**Abbreviation:** DOX/ELE Hyd NLCs, doxorubicin and β-elemene co-loaded, pH-sensitive nanostructured lipid carriers.

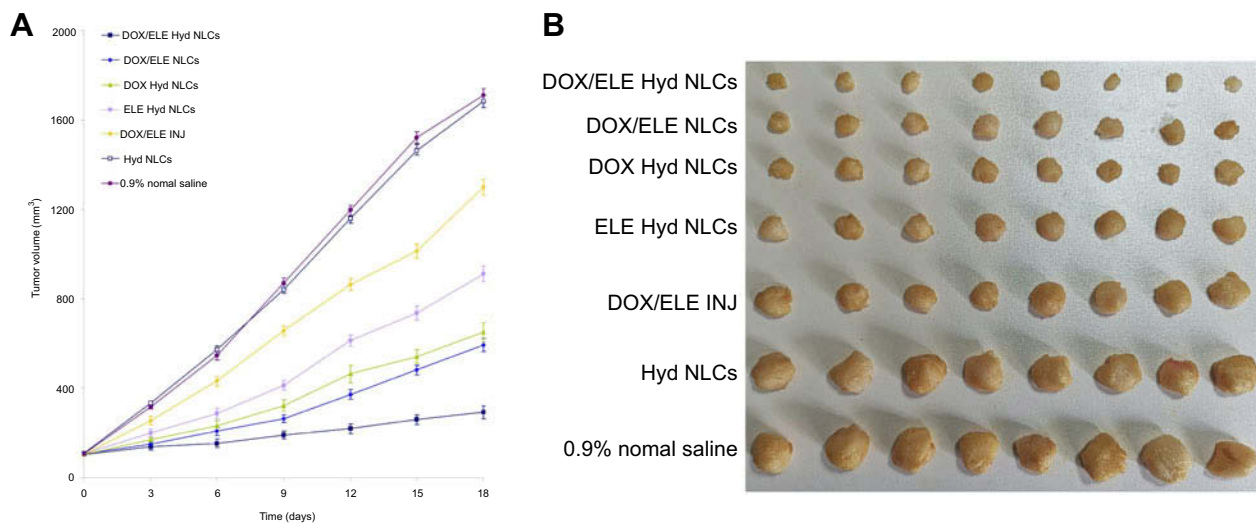


**Figure 8** In vivo anticancer activity presented as tumor growth curves (A) and tumor images (B) of each group. Data is presented as means ± SD, n=8.

**Abbreviation:** DOX/ELE Hyd NLCs, doxorubicin and β-elemene co-loaded, pH-sensitive nanostructured lipid carriers.

**Table 2** Tumor inhibition ratios (mean ± SD, n=3)

| Formulations                | DOX/ELE Hyd NLCs | DOX/ELE NLCs | DOX Hyd NLCs | ELE Hyd NLCs | DOX/ELE INJ |
|-----------------------------|------------------|--------------|--------------|--------------|-------------|
| Tumor inhibition ratios (%) | 82.9±3.7         | 65.4±3.2     | 61.9±4.1     | 46.7±2.6     | 24.1±2.1    |

**Abbreviations:** DOX/ELE Hyd NLCs, doxorubicin and β-elemene co-loaded, pH-sensitive nanostructured lipid carriers; INJ, injection.

loaded NLCs than injection groups may be explained as follows: the lipid structure on the surface of the NLCs are similar to the cell membrane, and they may improve the affinity of the systems and increase the drug delivery effect.<sup>42</sup> The sustained release behavior of NLCs may help with the delivery of the drugs to the tumor site, thus achieving the long-lasting antitumor effect in vivo. The tumor volume of DOX/ELE Hyd NLCs was significantly smaller compared with DOX/ELE NLCs, indicating that the pH-sensitive carriers have more remarkable tumor inhibition ability. DOX Hyd NLCs and ELE Hyd NLCs exhibited obviously high antitumor effect by suspending the growth of the tumor. However, they are less efficient than the double-drug co-loaded DOX/ELE Hyd NLCs, which have the synergy effect of the two drugs. These results indicate that DOX/ELE Hyd NLCs had greater lung tumor inhibition ability than DOX/ELE NLCs, DOX Hyd NLCs, ELE Hyd NLCs, and DOX/ELE IJN in vivo.

## Conclusion

In this study, we presented a promising approach to improve the efficiency of DOX and ELE into lung cancer cells and tumor site. The pH-sensitive, dual-drug co-loaded NLCs exhibited significantly enhanced cytotoxicity, profound tumor inhibition rate compared with the non pH-responsive NLCs, and single-drug-loaded NLCs. Since the synergistic effect of the drugs was found in this system, it would have the great potential to inhibit lung tumor cells and tumor growth in vivo.

## Acknowledgment

This study was funded by Jiangsu Young Medical Talent Fund (No. QNRC2016379).

## Disclosure

The authors report no conflicts of interest in this work.

## References

1. Torre LA, Siegel RL, Jemal A. Lung cancer statistics. *Adv Exp Med Biol*. 2016;893:1–19. doi:10.1007/978-3-319-24223-1\_1
2. Siegel RL, Miller KD, Jemal A. Cancer statistics, 2018. *CA Cancer J Clin*. 2018;68:7–30. doi:10.3322/caac.21442
3. Wakelee H, Kelly K, Edelman MJ. 50 years of progress in the systemic therapy of non-small cell lung cancer. *Am Soc Clin Oncol Educ Book*. 2014;177–189. doi:10.14694/EdBook\_AM.2014.34.177
4. Pérez-Herrero E, Fernández-Medarde A. Advanced targeted therapies in cancer: drug nanocarriers, the future of chemotherapy. *Eur J Pharm Biopharm*. 2015;93:52–79. doi:10.1016/j.ejpb.2015.03.018
5. Lee MS, Dees EC, Wang AZ. Nanoparticle-delivered chemotherapy: old drugs in new packages. *Oncology (Williston Park)*. 2017;31(3):198–208.
6. Estanqueiro M, Amaral MH, Conceição J, Sousa Lobo JM. Nanotechnological carriers for cancer chemotherapy: the state of the art. *Colloids Surf B Biointerfaces*. 2015;126:631–648. doi:10.1016/j.colsurfb.2014.12.041
7. Madane RG, Mahajan HS. Curcumin-loaded nanostructured lipid carriers (NLCs) for nasal administration: design, characterization, and in vivo study. *Drug Deliv*. 2016;23(4):1326–1334. doi:10.3109/10717544.2014.975382
8. Song S, Mao G, Du J, Zhu X. Novel RGD containing, temozolomide-loading nanostructured lipid carriers for glioblastoma multiforme chemotherapy. *Drug Deliv*. 2016;23(4):1404–1408. doi:10.3109/10717544.2015.1064186
9. Muller RH, Radtke M, Wissing SA. Solid lipid nanoparticles (SLN) and nanostructured lipid carriers (NLC) in cosmetic and dermatological preparations. *Adv Drug Deliv Rev*. 2002;54(Suppl 1):S131–155.
10. Liu Q, Li J, Pu G, Zhang F, Liu H, Zhang Y. Co-delivery of baicalin and doxorubicin by hyaluronic acid decorated nanostructured lipid carriers for breast cancer therapy. *Drug Deliv*. 2016;23(4):1364–1368. doi:10.3109/10717544.2015.1031295
11. Du J, Li L. Which one performs better for targeted lung cancer combination therapy: pre- or post-bombesin-decorated nanostructured lipid carriers? *Drug Deliv*. 2016;23(5):1799–1809. doi:10.3109/10717544.2015.1099058
12. Wang Y, Zhang H, Hao J, Li B, Li M, Xiuwen W. Lung cancer combination therapy: co-delivery of paclitaxel and doxorubicin by nanostructured lipid carriers for synergistic effect. *Drug Deliv*. 2016;23(4):1398–1403. doi:10.3109/10717544.2015.1055619
13. Taratula O, Kuzmov A, Shah M, Garbuzenko OB, Minko T. Nanostructured lipid carriers as multifunctional nanomedicine platform for pulmonary co-delivery of anticancer drugs and siRNA. *J Control Release*. 2013;171(3):349–357. doi:10.1016/j.jconrel.2013.04.018
14. Tan S, Wang G. Redox-responsive and pH-sensitive nanoparticles enhanced stability and anticancer ability of erlotinib to treat lung cancer in vivo. *Drug Des Devel Ther*. 2017;11:3519–3529. doi:10.2147/DDDT.S151422
15. Tran TH, Ramasamy T, Choi JY, et al. Tumor-targeting, pH-sensitive nanoparticles for docetaxel delivery to drug-resistant cancer cells. *Int J Nanomedicine*. 2015;10:5249–5262. doi:10.2147/IJN.S89584
16. Wang B, Peng XX, Sun R, et al. Systematic review of  $\beta$ -elemene injection as adjunctive treatment for lung cancer. *Chin J Integr Med*. 2012;18(11):813–823. doi:10.1007/s11655-012-1271-9
17. Zhai B, Zeng Y, Zeng Z, et al. Drug delivery systems for elemene, its main active ingredient  $\beta$ -elemene, and its derivatives in cancer therapy. *Int J Nanomedicine*. 2018;13:6279–6296. doi:10.2147/IJN.S174527
18. Liu Y, Jiang ZY, Zhou YL, et al.  $\beta$ -elemene regulates endoplasmic reticulum stress to induce the apoptosis of NSCLC cells through PERK/IRE1 $\alpha$ /ATF6 pathway. *Biomed Pharmacother*. 2017;93:490–497. doi:10.1016/j.biopha.2017.06.073
19. Li J, JunYu LA, Wang Y.  $\beta$ -elemene against human lung cancer via up-regulation of P53 protein expression to promote the release of exosome. *Lung Cancer*. 2014;86(2):144–150. doi:10.1016/j.lungcan.2014.08.015
20. Lin L, Li L, Chen X, Zeng B, Lin T. Preliminary evaluation of the potential role of  $\beta$ -elemene in reversing erlotinib-resistant human NSCLC A549/ER cells. *Oncol Lett*. 2018;16(3):3380–3388. doi:10.3892/ol.2018.8980
21. Manh Hung LV, Song YW, Cho SK. Effects of the combination of gliotoxin and adriamycin on the adriamycin-resistant non-small-cell lung cancer A549 cell line. *Mar Drugs*. 2018;16(4). doi:10.3390/md16040105

22. Cai Z, Zhang H, Wei Y, Wei Y, Xie Y, Cong F. Reduction- and pH-sensitive hyaluronan nanoparticles for delivery of iridium(III) anticancer drugs. *Biomacromolecules*. 2017;18(7):2102–2117. doi:10.1021/acs.biomac.7b00445
23. Zhang Y, Zhang P, Zhu T. Ovarian carcinoma biological nanotherapy: comparison of the advantages and drawbacks of lipid, polymeric, and hybrid nanoparticles for cisplatin delivery. *Biomed Pharmacother*. 2018;3(109):475–483.
24. Shi F, Yang G, Ren J, Guo T, Du Y, Feng N. Formulation design, preparation, and in vitro and in vivo characterizations of  $\beta$ -elemene-loaded nanostructured lipid carriers. *Int J Nanomedicine*. 2013;8:2533–2541. doi:10.2147/IJN.S46578
25. Cui T, Zhang S, Sun H. Co-delivery of doxorubicin and pH-sensitive curcumin prodrug by transferrin-targeted nanoparticles for breast cancer treatment. *Oncol Rep*. 2017;37(2):1253–1260. doi:10.3892/or.2017.5345
26. Qiu J, Cai G, Liu X, Ma D.  $\alpha(v)\beta(3)$  integrin receptor specific peptide modified, salvianolic acid B and panax notoginsenoside loaded nanomedicine for the combination therapy of acute myocardial ischemia. *Biomed Pharmacother*. 2017;96:1418–1426. doi:10.1016/j.biopha.2017.10.086
27. Li S, Wang L, Li N, Liu Y, Su H. Combination lung cancer chemotherapy: design of a pH-sensitive transferrin-PEG-Hz-lipid conjugate for the co-delivery of docetaxel and baicalin. *Biomed Pharmacother*. 2017;95:548–555. doi:10.1016/j.biopha.2017.08.090
28. Li C, Li H, Wang Q, et al. pH-sensitive polymeric micelles for targeted delivery to inflamed joints. *J Control Release*. 2017;246:133–141. doi:10.1016/j.jconrel.2016.12.027
29. Yan J, Wang Y, Jia Y, et al. Co-delivery of docetaxel and curcumin prodrug via dual-targeted nanoparticles with synergistic antitumor activity against prostate cancer. *Biomed Pharmacother*. 2017;88:374–383. doi:10.1016/j.biopha.2016.12.138
30. Zhang J, Xiao X, Zhu J, et al. Lactoferrin- and RGD-comodified, temozolomide and vincristine-co-loaded nanostructured lipid carriers for gliomatosis cerebri combination therapy. *Int J Nanomedicine*. 2018;13:3039–3051. doi:10.2147/IJN.S161163
31. Tan S, Wang G. Lung cancer targeted therapy: folate and transferrin dual targeted, glutathione responsive nanocarriers for the delivery of cisplatin. *Biomed Pharmacother*. 2018;102:55–63. doi:10.1016/j.biopha.2018.03.046
32. Wang Z, Wei Y, Fang G, et al. Colorectal cancer combination therapy using drug and gene co-delivered, targeted poly(ethylene glycol)- $\epsilon$ -poly(caprolactone) nanocarriers. *Drug Des Devel Ther*. 2018;12:3171–3180. doi:10.2147/DDDT.S175614
33. Nie Y, Günther M, Gu Z, Wagner E. Pyridylhydrazone-based PEGylation for pH-reversible lipopolyplex shielding. *Biomaterials*. 2011;32(3):858–869. doi:10.1016/j.biomaterials.2010.09.032
34. Jelezova I, Drakalska E, Momekova D, et al. Curcumin loaded pH-sensitive hybrid lipid/block copolymer nanosized drug delivery systems. *Eur J Pharm Sci*. 2015;78:67–78. doi:10.1016/j.ejps.2015.07.005
35. Yu D, Li W, Zhang Y, Zhang B. Anti-tumor efficiency of paclitaxel and DNA when co-delivered by pH responsive ligand modified nanocarriers for breast cancer treatment. *Biomed Pharmacother*. 2016;83:1428–1435. doi:10.1016/j.biopha.2016.08.061
36. Yan J, Wang Y, Zhang X, Liu S, Tian C, Wang H. Targeted nanomedicine for prostate cancer therapy: docetaxel and curcumin co-encapsulated lipid-polymer hybrid nanoparticles for the enhanced anti-tumor activity in vitro and in vivo. *Drug Deliv*. 2016;23(5):1757–1762. doi:10.3109/10717544.2015.1069423
37. Liang Y, Tian B, Zhang J, et al. Tumor-targeted polymeric nanostructured lipid carriers with precise ratiometric control over dual-drug loading for combination therapy in non-small-cell lung cancer. *Int J Nanomedicine*. 2017;12:1699–1715. doi:10.2147/IJN.S121262
38. Dong T, Chen N, Ma X, et al. The protective roles of L-borneolum, D-borneolum and synthetic borneol in cerebral ischaemia via modulation of the neurovascular unit. *Biomed Pharmacother*. 2018;102:874–883. doi:10.1016/j.biopha.2018.03.087
39. Fang XB, Zhang JM, Xie X, et al. pH-sensitive micelles based on acid-labile pluronic F68-curcumin conjugates for improved tumor intracellular drug delivery. *Int J Pharm*. 2016;502(1–2):28–37. doi:10.1016/j.ijpharm.2016.01.029
40. Baek JS, Cho CW. A multifunctional lipid nanoparticle for co-delivery of paclitaxel and curcumin for targeted delivery and enhanced cytotoxicity in multidrug resistant breast cancer cells. *Oncotarget*. 2017;8(18):30369–30382. doi:10.18632/oncotarget.16153
41. Liu J, Cheng H, Han L, et al. Synergistic combination therapy of lung cancer using paclitaxel- and triptolide-co-loaded lipid-polymer hybrid nanoparticles. *Drug Des Devel Ther*. 2018;12:3199–3209. doi:10.2147/DDDT.S172199
42. Wang G, Wang Z, Li C, et al. RGD peptide-modified, paclitaxel prodrug-based, dual-drugs loaded, and redox-sensitive lipid-polymer nanoparticles for the enhanced lung cancer therapy. *Biomed Pharmacother*. 2018;106:275–284. doi:10.1016/j.biopha.2018.06.137
43. Ding Y, Sun D, Wang GL, et al. An efficient PEGylated liposomal nanocarrier containing cell-penetrating peptide and pH-sensitive hydrazone bond for enhancing tumor-targeted drug delivery. *Int J Nanomedicine*. 2015;10:6199–6214. doi:10.2147/IJN.S92519

## Drug Design, Development and Therapy

### Publish your work in this journal

Drug Design, Development and Therapy is an international, peer-reviewed open-access journal that spans the spectrum of drug design and development through to clinical applications. Clinical outcomes, patient safety, and programs for the development and effective, safe, and sustained use of medicines are a feature of the journal, which has also

Submit your manuscript here: <https://www.dovepress.com/drug-design-development-and-therapy-journal>

been accepted for indexing on PubMed Central. The manuscript management system is completely online and includes a very quick and fair peer-review system, which is all easy to use. Visit <http://www.dovepress.com/testimonials.php> to read real quotes from published authors.

Dovepress